NREL
NATIONAL RENEWABLE ENERGY LABORATORY

Sub-Hourly Impacts of High Solar Penetrations in the Western United States

Preprint

D. Lew, G. Brinkman, E. Ibanez, M. Hummon, B.-M. Hodge, and M. Heaney
National Renewable Energy Laboratory

J. King
RePPAE

To be presented at the 2nd Annual International Workshop on Integration of Solar Power into Power Systems Conference
Lisbon, Portugal
November 12–13, 2012

Conference Paper
NREL/CP-5500-56171
September 2012

Contract No. DE-AC36-08GO28308

Available electronically at http://www.osti.gov/bridge

Available for a processing fee to U.S. Department of Energy
and its contractors, in paper, from:

U.S. Department of Energy
Office of Scientific and Technical Information
P.O. Box 62
Oak Ridge, TN 37831-0062
phone: 865.576.8401
fax: 865.576.5728
email: mailto:reports@adonis.osti.gov

Available for sale to the public, in paper, from:

U.S. Department of Commerce
National Technical Information Service
5285 Port Royal Road
Springfield, VA 22161
phone: 800.553.6847
fax: 703.605.6900
email: orders@ntis.fedworld.gov
online ordering: http://www.ntis.gov/help/ordermethods.aspx

Cover Photos: (left to right) PIX 16416, PIX 17423, PIX 16560, PIX 17613, PIX 17436, PIX 17721

Printed on paper containing at least 50% wastepaper, including 10% post consumer waste.

Sub-Hourly Impacts of High Solar Penetrations in the Western United States

Debra Lew, Greg Brinkman, Anthony Florita, Michael Heaney,
Bri-Mathias Hodge, Marissa Hummon, Eduardo Ibanez
National Renewable Energy Laboratory
Golden, CO 80401; USA
debra.lew@nrel.gov

Jack King
RePPAE
Wexford, PA 15090; USA

***Abstract*—Until recently, it has been difficult to study the impacts of significant penetrations of hypothetical, utility-scale solar photovoltaic (PV) plants over large geographic regions. This was because of the lack of credible data to simulate the output of these plants with appropriate spatial and temporal correlation, especially on a sub-hourly basis. In the Western Wind and Solar Integration Study Phase 2 (WWSIS2), we used new techniques to synthesize sub-hourly high-resolution solar power output for PV rooftops, utility-scale PV, and concentrating solar power (CSP). This allowed us to examine implications of 25% solar (60/40 split of PV and CSP) and 8% wind. In this paper, we present results of analysis on the sub-hourly impacts of high solar penetrations. Extreme event analysis showed that most of the large ramps were because of sunrise and sunset events, which have a significant predictability component. Variability in general was much higher with high penetrations of solar than with high penetrations of wind. Reserve methodologies that had already been developed for wind were therefore modified to take into account the predictability component of solar variability. Significantly less transmission was required for high solar penetrations than wind and significantly less curtailment occurred in the high solar cases.**

Keywords-solar; integration; wind; variability; uncertainty; statistics; reserves

I. INTRODUCTION

There is considerable knowledge and understanding of the integration of wind power into power systems [1–3]. In some ways, integration of solar power is very similar to that of wind power. Solar is variable, meaning that the resource varies seasonally, diurnally, and on a sub-hourly timescale. It is also uncertain, meaning that the resource cannot be perfectly forecasted in the day-ahead, hour-ahead, or even 5-min ahead time frame. The power system must be designed to provide resource adequacy and to have sufficient reserves to accommodate this variability and uncertainty.

However, solar differs from wind in some remarkable ways. There is a large predictability component to solar plant output because of the predictable path of the sun through the sky. Solar output also results in significant ramps because of sunrise and sunset, especially with single- and double-axis tracking technologies. Although these ramps may be predictable, the system operator still needs to balance the system.

The Western Wind and Solar Integration Study Phase 1 (WWSIS1) examined the operational impacts of up to 30% wind and 5% solar in the WestConnect region of the Western Interconnection (WI) of the United States [4]. Solar penetration levels in WWSIS1 were limited to 5% because solar data synthesis was not yet sophisticated enough to create credible scenarios of high solar penetrations. Additionally, production simulation modeling was conducted on an hourly time step because of limitations with commercial software tools. Despite the lack of good data, a high-level analysis was conducted using rooftop PV data to start to understand issues with high solar penetrations [5–6].

Because of new developments in synthesizing sub-hourly, utility-scale photovoltaic (PV) plant output, WWSIS2 was able to address high solar penetrations in detail as well as compare solar to wind. As a result, WWSIS2 investigated up to 25% solar energy penetration across the WI, with an examination of utility-scale as well as rooftop PV plants. WWSIS2 also compared the operational impacts of high wind versus high solar penetrations. Finally, WWSIS2 incorporated new data on wear-and-tear costs and emissions to understand the impacts of solar and wind power on fossil-fired generators. In this paper, we report on the impacts of solar in WWSIS2, compare wind and solar impacts on the grid, and examine the sub-hourly impacts of solar power in the WI.

II. DATA INPUTS

WWSIS2 modeled the future year of 2020 with load projected to that year. The weather and load shapes from 2004 to 2006 were modeled to examine interannual variability. The base model for WWSIS2 was the Western Electricity Coordinating Council (WECC) Transmission Expansion Policy Planning Committee (TEPPC) Portfolio Case #1 (PC1) 2020, which has been widely vetted by WECC stakeholders [7]. There is a tradeoff between zonal granularity and model complexity and run time. We used the 20 WECC Loads and Resources Subcommittee zones, which are an approximation of the nearly 40 balancing areas that make up the WI.

Although the WI includes parts of Canada and Mexico, we do not have sufficient solar and wind data to model high penetrations of solar and wind in those countries. Therefore, we focused on solar and wind build-outs in the U.S. portion of the WI and discussed energy penetration levels as a percentage of the U.S. load.

A. *Solar Plant Output Data Synthesis*

To model the hypothetical impact of up to 25% solar energy penetration, solar power plant outputs for hypothetical plants must be synthesized. These plant outputs should show temporal and spatial correlation as well as realistic variability over various timescales [8]. A new technique was developed to synthesize PV and concentrating solar power (CSP) power plant output with realistic variability down to the 1-min timescale [9]. This methodology converted spatial variability from surrounding satellite images into sub-hourly temporal variability. The sub-hourly irradiation was converted to power using the National Renewable Energy Laboratory's (NREL's) System Advisor Model [10]. This new data set was validated against high-resolution measurements of irradiance and PV power output [11].

The solar plants modeled for WWSIS2 were:

- Rooftop PV—aggregated, distributed-generation PV on residential and commercial rooftops;
- Population-weighted PV—utility-scale PV plants in urban and suburban areas (e.g., airport installations and other MW-scale installations);
- Best-resource-located PV—utility-scale PV plants in desert and remote locations where the resource is exceptional; and
- CSP—utility-scale power plants with 6 h thermal storage. The storage was dispatched using the commercial PLEXOS production simulation model.

B. *Solar Forecast Data Synthesis*

In addition to synthesizing hypothetical solar power plant outputs, we needed to understand solar uncertainty, or forecast error. Therefore, we needed to synthesize solar plant forecasts for the same hypothetical plants. Our production simulation modeling utilized a day-ahead, 4-h ahead, and real-time market, so we synthesized day-ahead, 4-h ahead, and 1-h ahead solar forecasts for each plant.

Day-ahead solar forecasts were based on the WWSIS1 solar forecast synthesis conducted by 3TIER based on Numerical Weather Prediction simulations [11–12]. Four-h-ahead solar forecasts were modeled using 2-h persistence of cloudiness because it was found that with wind forecast errors, 2-h persistence matched 4-h forecast errors reasonably well. One-h-ahead forecasts were modeled using 1-h persistence of cloudiness. A persistence forecast would have ignored the fact that the sun traces a predictable path through the sky. Because we wanted to incorporate this predictability into our synthesized forecasts, we instead used persistence of cloudiness.

(a)

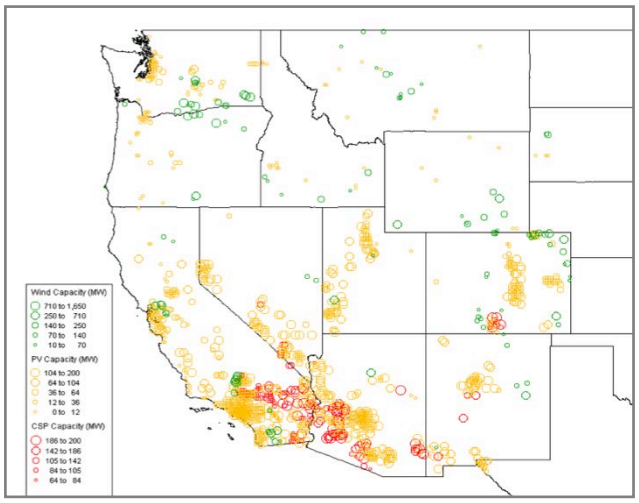

(b)

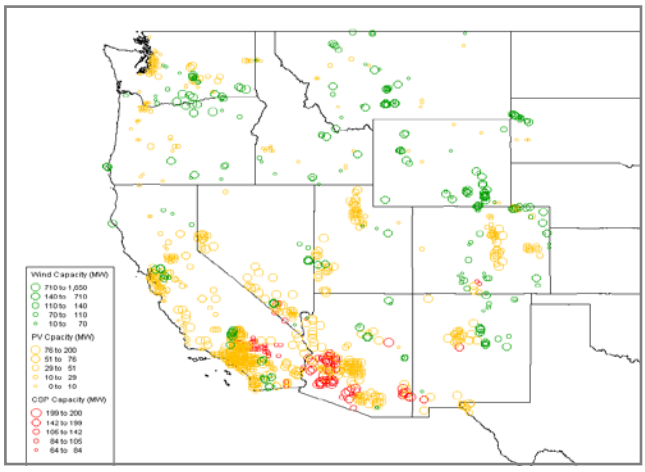

(c)

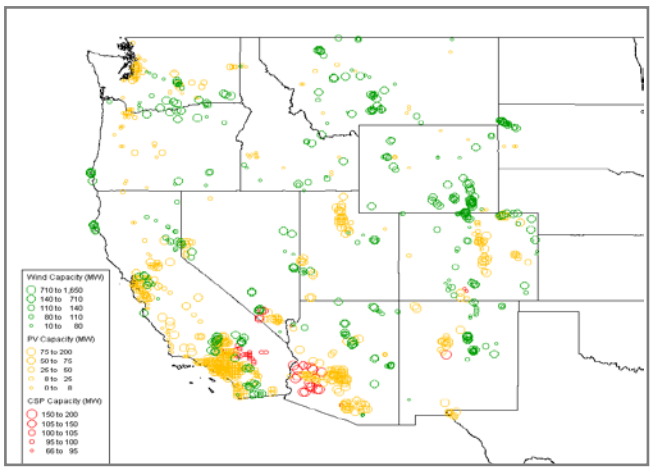

Figure 1. Siting of PV, CSP, and wind plants for the (a) High-Solar, High-Mix, and (c) High-Wind Scenarios. Wind, PV and CSP plants are shown in green, yellow, and red circles, respectively, with larger plants depicted with larger circles.

III. Scenarios

The reference and three high-renewables scenarios defined and sited for the study were:

- Reference—8% wind and 3% solar. This scenario was based on the WECC TEPPC 2020 PC1 base case scenario, which included enough renewables so that western states met their 2020 renewable portfolio standards targets.
- High-Solar—25% solar and 8% wind
- High-Wind—25% wind and 8% solar
- High-Mix—16.5% wind and 16.5% solar

All solar portfolios were comprised of the following solar technologies:

- 24% rooftop PV;
- 12% population-weighted PV;
- 24% best-resource-located PV; and
- 40% CSP with storage.

The scenarios are shown in Fig. 1. NREL's Regional Energy Deployment System model [13] was used to select sites according to criteria above. Fig. 2 shows the siting for the High-Solar Scenario. The size of the circle depicts the capacity of the solar or wind plant.

IV. Statistical Analysis

Statistical and extreme event analysis was undertaken to examine the variability of solar, wind, and net load (defined as load minus solar minus wind) on a subregional and regional basis.

A. Geographic Diversity

Fig. 2 shows the smoothing of solar output with increasing aggregation of solar sites throughout Southern California. At the individual plant level, cloud events were seen with the fast ramps in the PV plant output. These events smoothed out as output from 6 and then 25 plants were aggregated. At the subregional level, individual cloud events could not be discerned.

We used this same approach to compare rooftop PV, utility-scale PV, and wind in Fig. 3. Total aggregate capacity was defined similarly, as increasing concentric circles that included larger areas and higher capacity. Variability was defined here as one standard deviation of the hourly change in output. The utility-scale PV and wind profiles started with relatively high variability when a few plants were examined. Wind variability dropped off rapidly as plants were aggregated, with the normalized variability leveling off at about 1%. Utility-scale PV variability leveled off at slightly less than 4%. Rooftop PV, already an aggregation of many small plants, showed relatively little benefit as increasing amounts were aggregated over larger areas.

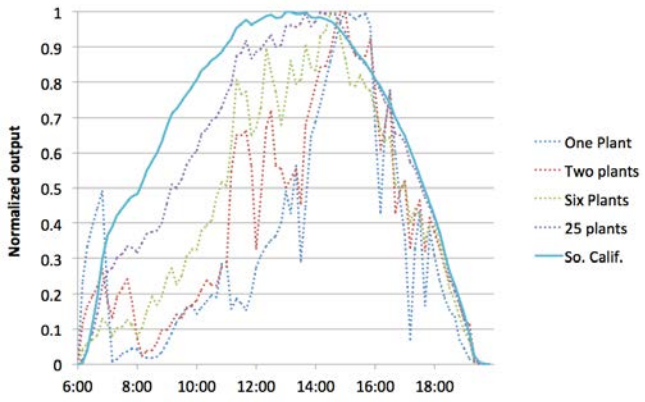

Figure 2. Normalized PV output for increasing aggregation of PV plants in Southern California for a partly cloudy day.

(a)

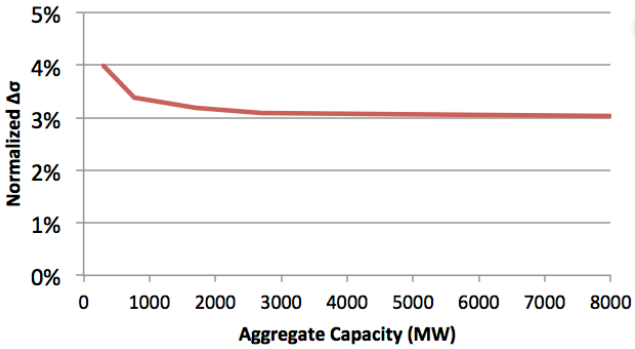

(b)

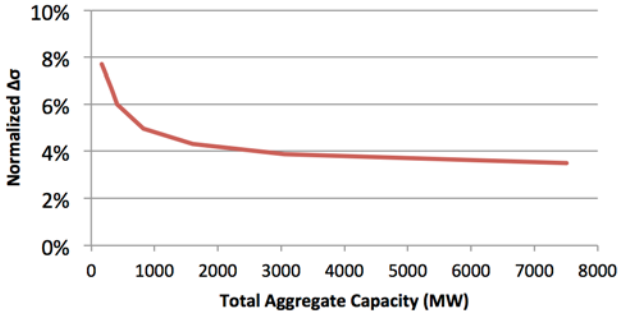

(c)

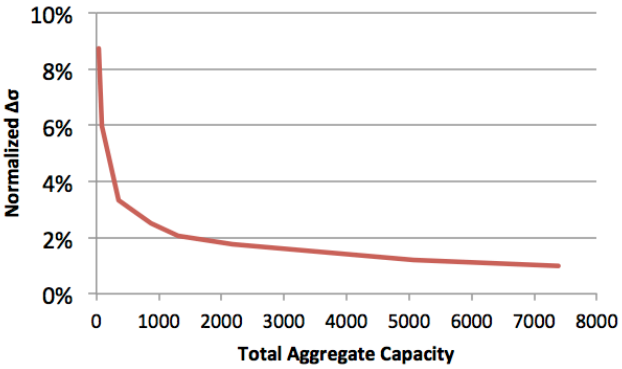

Figure 3. Normalized variability as a function of aggregate capacity for (a) rooftop PV, (b) utility-scale PV and (c) wind. Note the difference in y-axis scales.

B. Diurnal Variability

Fig. 4 (a) shows the diurnal variability of the WI load. On average, the morning load pickup was followed by a gradual rise to an evening peak, with a nighttime minimum. The hourly change in load is also depicted, which experienced significant variability in the late-afternoon hours.

(a)

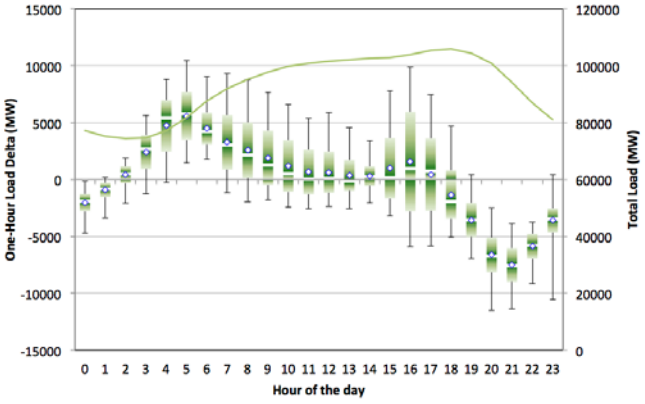

(b)

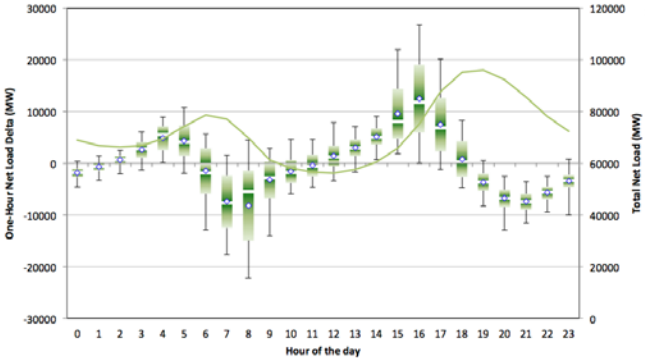

(c)

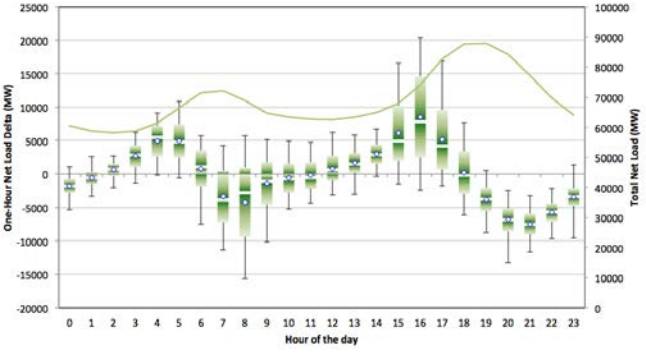

(d)

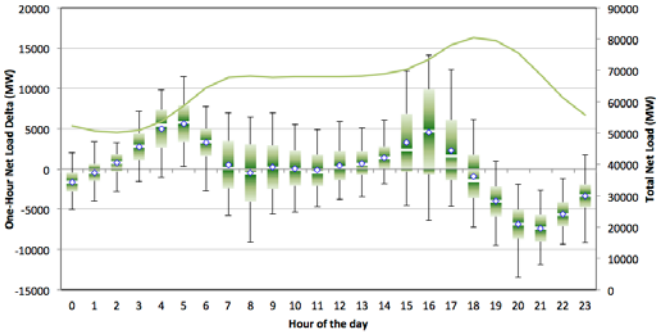

Figure 4. (a) Diurnal variability of the load (green line) and the hourly change in load (white line—median; diamond—mean; bar—standard deviation; whiskers—minimum and maximum). Diurnal variability of the net load and hourly change in net load for the (b) High-Solar, (c) High-Mix, and (d) High-Wind Scenarios. Note the difference in y-axis scales. CSP was not included in these plots.

Fig. 4 (b) shows the net load variability of the High-Solar Scenario. The high-solar output during midday led to a double peak in net load, once in the morning and again in the evening. The hourly net load delta shows that the variability increased considerably during sunrise and sunset. For the High-Mix and High-Wind Scenarios, as the solar penetration decreased and the wind increased, the double peak in net load disappeared, with the net load shape being similar to the load shape, depressed by about 10,000 MW to 15,000 MW.

C. Hourly Variability

The hourly variability was also examined. Fig. 5 (a) shows the hourly load change versus the hourly wind change for the High-Wind Scenario (25% wind). Fig. 5 (b) shows the hourly load change versus the hourly PV change for the High-Solar Scenario (15% PV; CSP is not shown) for 8,760 h of the year 2006. For these hourly variability plots, it is important to note that the top right and bottom left quadrants show the hours when solar and wind moved in the same direction as the load, thus helping the power system meet load. The top left quadrant shows increased solar and wind while load decreased. Operators may be able to curtail solar and wind production to balance load. The bottom right quadrant depicts the difficult hours for the operator, when solar and wind decreased while load increased. The bottom right quadrant extrema are particularly challenging. Ensuring enough up-reserves during these hours is critical.

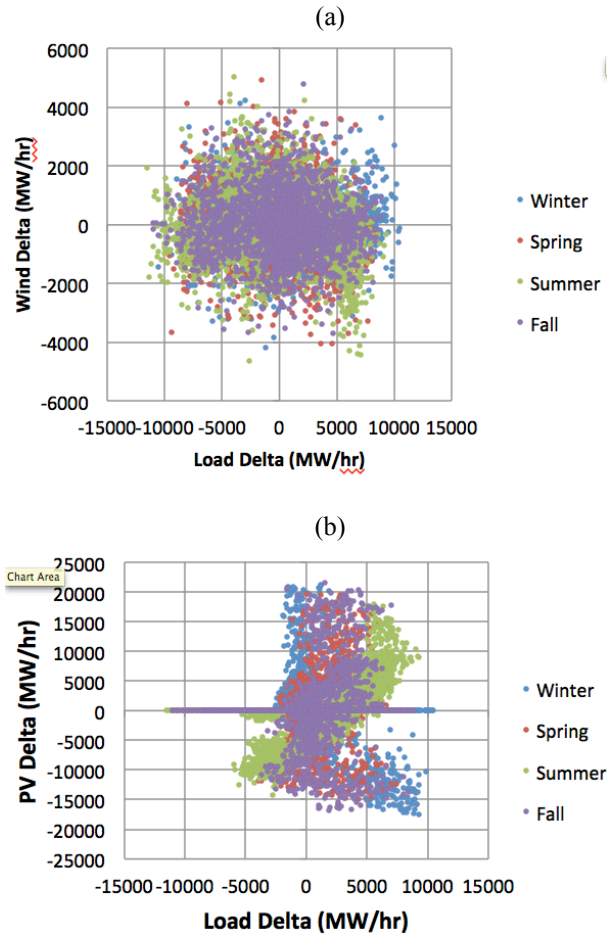

Figure 5. (a) Hourly load change versus hourly wind production change for the High-Wind Scenario and (b) hourly load change versus hourly PV production change for the High-Solar Scenario. Note the difference in y-axis scales. The different colors depict the different seasons.

Fig. 5 (a) shows that wind variability was generally uncorrelated with both load variability and season. In contrast, Fig. 5 (b) shows that there were a significant number of hours where PV helped the load, during morning load rise and as the sun rose. In the winter, however, there were many hours when load was increasing while PV output was decreasing. This is because of the mismatch of the evening load pickup while the sun set. Fig. 5 (b) also shows a large number of nighttime hours where the PV change was zero.

Fig. 6 (a) through (c) show the hourly load change versus the hourly variability of the variable generation (VG) output (excluding the CSP) for the three high-renewables scenarios for 8,760 h of the year 2006. The hourly variability of the VG in the High-Solar Scenario (note the different y-axis scales) was much greater than that of the High-Mix and far greater than that of the High-Wind Scenarios. The maximum hourly VG change in the High-Solar Scenario was =22,000 MW/h and -17,000 MW/h, which was significantly higher than the +8,000 MW/h and -7,900 MW/h of the High-Wind Scenario. This illustrates the significant variability that must accommodate high solar penetrations.

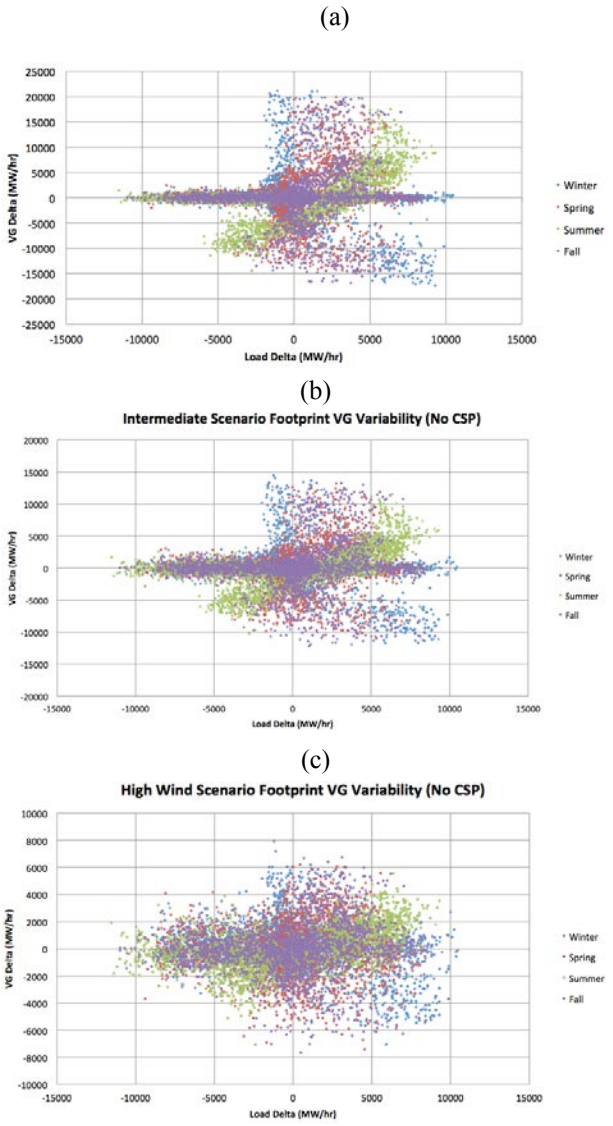

Figure 6. Hourly load change versus hourly VG production change for the (a) High-Solar Scenario, (b) High-Mix Scenario, and (c) High-Wind Scenario for 2006. Note the difference in y-axis scales. CSP was not included in the VG in this graph.

D. Sub-Hourly Variability

At the 5-min level, correlations between changes in load and changes in VG output were similar to that at the hourly timescale, as shown in Fig. 7. Again, the y-axis scales on the High-Solar and High-Wind Scenarios were different and significantly more 5-min variability occurred in the High-Solar Scenario.

Statistics for the 5-min changes in net load are shown for selected subregions in Table I. Subregions in the north, such as Columbia Grid and the Northern Tier Transmission Group, have relatively less solar capacity and showed relatively modest changes in the standard deviation of 5-min changes in net load and the minimum and maximum changes for both the High-Solar and High-Wind Scenarios. Subregions in the south, such as the California Independent System Operator and WestConnect, have much higher solar capacities, and WestConnect in particular has a particularly high solar penetration level. The result of this is that the 5-min changes

in net load were significantly impacted in the High-Solar Scenario.

The tail events of the distribution are shown more clearly in Fig 9. The High-Wind Scenario had little impact on the maximum and minimum 5-min changes in net load but did increase the number of extreme events from load alone.

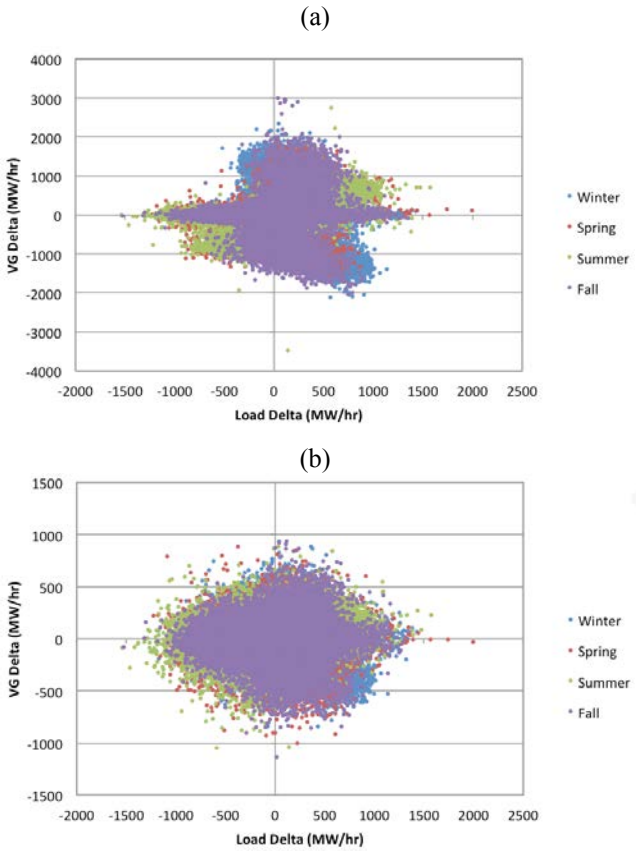

Figure 7. Five-min changes in load versus 5-min changes in VG output for (a) High-Solar and (b) High-Wind Scenarios. Note the difference in y-axis scales.

TABLE I. STATISTICS FOR 5-MIN CHANGES IN NET LOAD FOR THE HIGH-SOLAR SCENARIO FOR 2006 FOR THE WI FOOTPRINT AND SELECTED SUBREGIONS

	Columbia Grid	NTTG	West Connect	CAISO	Footprint
Sigma (MW)					
Load-alone	65	59	153	145	358
High-Solar Scenrio	76	80	312	183	548
High-Wind Scenario	78	82	187	150	390
Max Neg Delta (MW)					
Load-alone	-712	-885	-1084	-916	-1541
High-Solar Scenrio	-739	-882	-1771	-961	-2966
High-Wind Scenario	-739	-858	-1289	-901	-1879
Max Pos Delta (MW)					
Load-alone	538	722	1401	957	1991
High-Solar Scenrio	576	726	2090	1290	3611
High-Wind Scenario	633	760	1388	902	2020
No. Drops < 3 * Ld Sigma					
Load-alone	103	146	471	177	97
High-Solar Scenrio	590	1238	5081	575	1596
High-Wind Scenario	736	1859	875	204	219
No. Rises > 3* Ld Sigma					
Load-alone	1011	394	260	244	174
High-Solar Scenrio	1499	2066	7296	2015	3973
High-Wind Scenario	1632	1816	1352	915	791

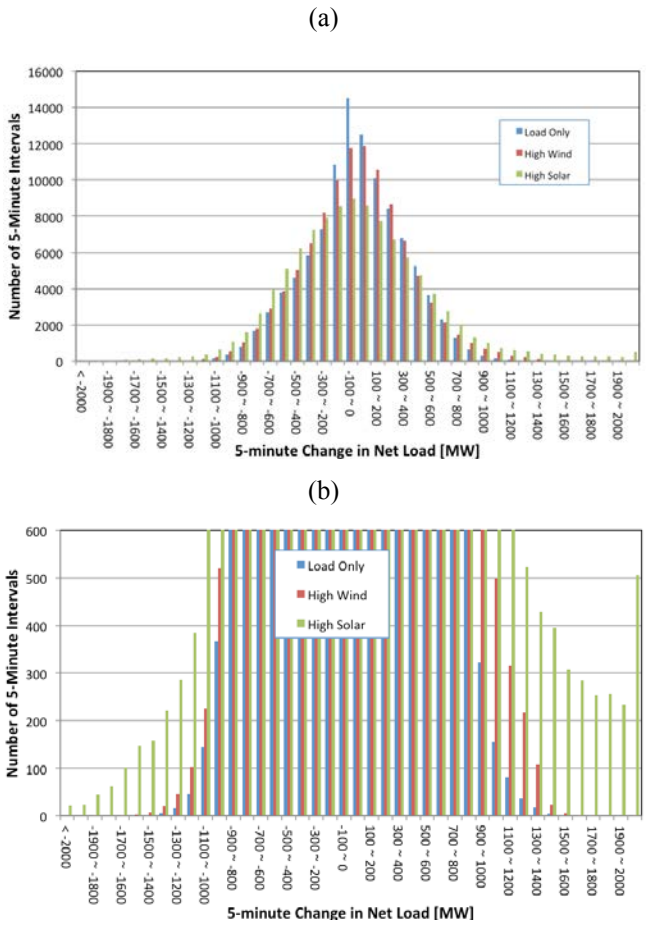

Figure 8. Histogram of 5-min changes in net load for (blue) load-only, (red) High-Wind, and (green) High-Solar Scenarios. (b) is an expanded view of the distribution tails.

The High-Solar Scenario both further increases the number of extreme events and causes them to be more extreme.

This increased variability must be managed by adequate up- and down-reserve margins. As mentioned above, the large predictability component of the solar variability means that operators may be in a position to plan for some of this variability. Wind flexibility reserve requirements are typically based on analysis of wind variability [16]. Solar reserve requirements based on the same analytical techniques would result in holding too much reserves, which would be costly. For WWSIS2, a methodology was developed to calculate flexibility reserve requirements based on the unpredictable component of solar variability [17].

V. TRANSMISSION EXPANSION

To bring resources to load, we expanded transmission using iterative load flows in PLEXOS. Forty-four transmission paths were considered at a zonal level so that collector systems did not need to be designed for this study. Nodal transmission build-outs may need to be considered in future analyses to examine details of congestion and flows. Transmission expansion focused on increasing capabilities of existing paths.

We developed a methodology to expand capabilities on existing transmission paths by running the four scenarios in

PLEXOS for a full year and examining annual average shadow prices across interfaces. We "built" 500 MW of additional transmission across interfaces whose annual average shadow prices exceeded some cutoff value. We then iterated and re-ran the revised scenario with the additional transmission in PLEXOS and added more transmission as appropriate until shadow prices no longer exceeded the cutoff value.

We tested cutoff values from $5/MWh to $20/MWh. These were consistent with the very rough estimate of transmission costs of $1,600/MW-mile for 250 miles of new transmission with a $0.11 fixed charge rate.

Fig. 9 (a) shows the initial transmission capacities and 9 (b) and 9 (c) show transmission capacities for a $20/MWh and $5/MWh cutoff value. The $5/MWh value resulted in 10,000 MW of additional transmission than the 5,000 MW in the $20/MWh value. This additional transmission resulted in additional production cost savings and reduced curtailment, as shown in Table II.

(a)

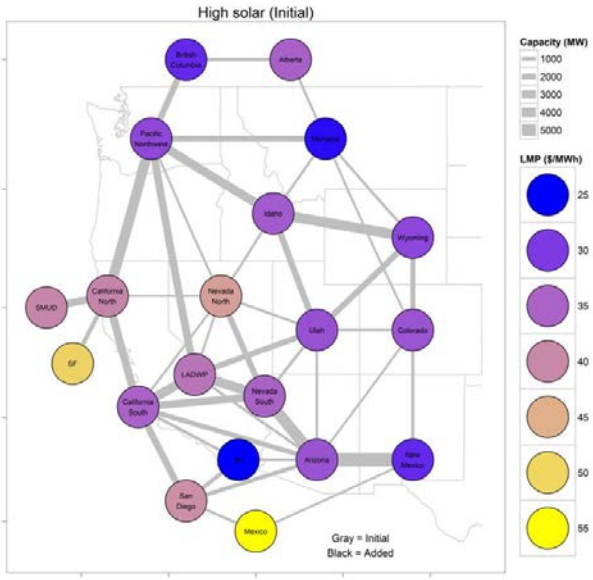

(b)

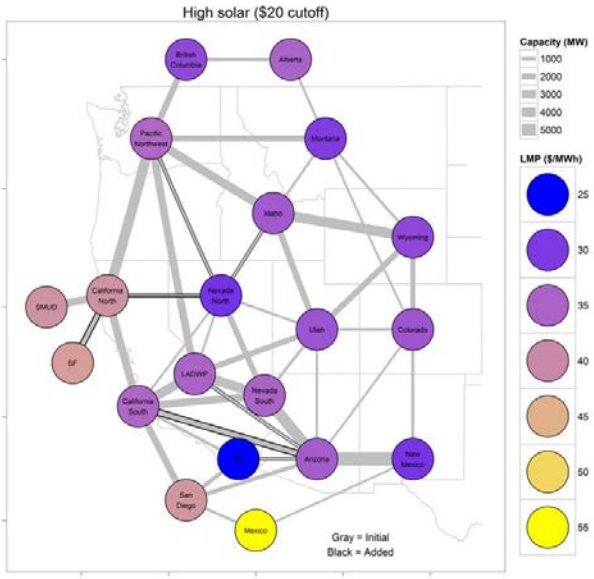

(c)

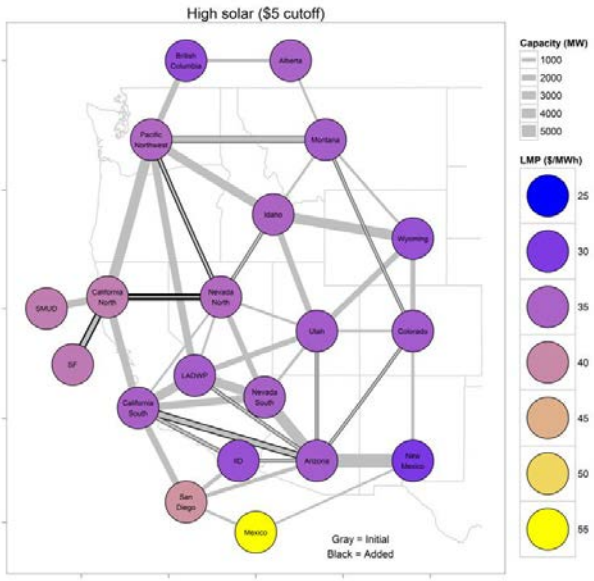

Figure 9. Iterative transmission capacities for the High-Solar Scenario showing (a) initial and final interface capabilities for (b) the $20 cutoff, and (c) the $5 cutoff shadow price. Locational marginal price is shown by the colors of each zone. The transmission capacity for major interfaces is shown by the width of the grey lines. New transmission capacity is shown by the width of the black lines.

Fig. 10 highlights some of the metrics used to evaluate the transmission build-outs for the scenarios. Fig. 10 (a) shows the production cost savings for each scenario as a function of cutoff shadow price and transmission MW built. The transmission built in the High-Solar Scenario at the $5/MWh cutoff shadow price was 10,000 MW, which was comparable to the transmission built in the High-Wind Scenario at the $10/MWh cutoff shadow price. That 10,000 MW of transmission in the High-Wind Scenario saves $923M/yr, however, which is about 50% higher than the $638M/yr saved in the High-Solar Scenario.

TABLE II. TRANSMISSION BUILD-OUT FOR THE HIGH-SOLAR SCENARIO

	Initial	*$20 Cutoff*	*$5 Cutoff*
Cumulative additional transmission capacity [MW]	0	5,000	10,000
Cumulative transmission annualized cost [M$/yr]	0	220	440
Production cost [B$/yr]	11.5	11.0	10.9
Cumulative production cost savings [M$/yr]		487	638
Average benefit/cost ratio		2.22	1.45
Curtailment [TWh]	4.7	1.6	1.3
Curtailment as fraction of potential wind and solar production	0.018	0.006	0.005
Transmission cost per MWh curtailment savings [$/MWh]		70.3	129.5

Curtailment decreased with expanded transmission. Fig. 10 (b) shows the curtailment as a function of cutoff shadow price and transmission MW built. Because solar peaks midday and wind is often stronger at night, wind curtailment is much greater than solar curtailment, even as transmission is built out for the High-Wind Scenario.

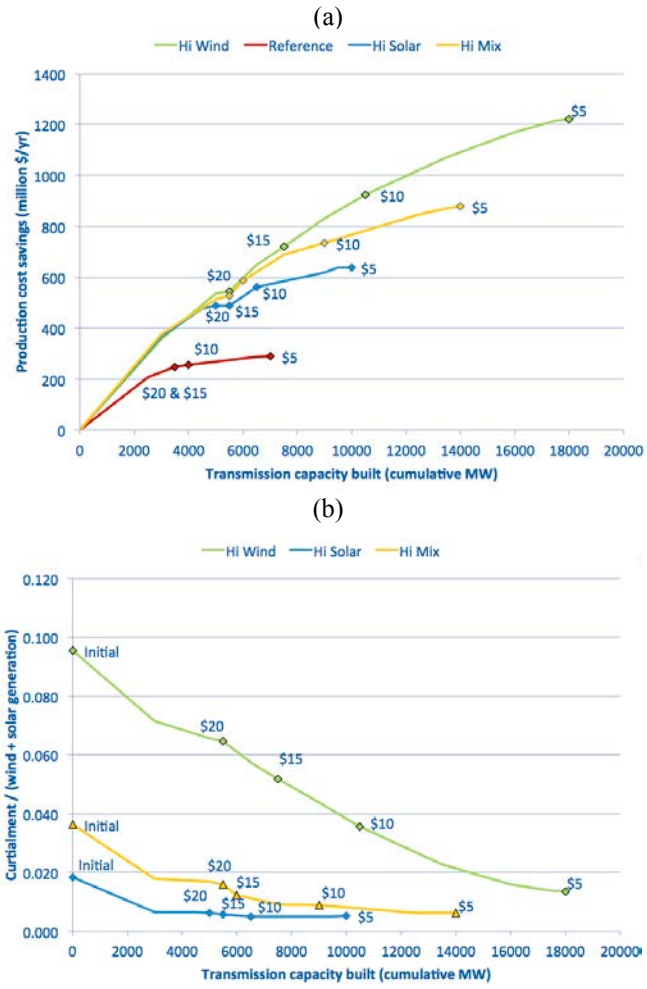

Figure 10. Comparison of transmission build-out metrics for reference, High-Solar, High-Wind, and High-Mix Scenarios, showing (a) production cost savings versus MW built and (b) curtailment versus MW built.

VI. CONCLUSIONS

High penetrations of solar power pose different issues than wind for the power system. Solar has some advantages over wind. It is more coincident with load and tends to provide output throughout the year, whereas wind typically dips in the summer and during summer peak. On the other hand, net load variability increases significantly more with solar than for the same annual energy penetration from wind. However, this variability contains a predictable (sunrise and sunset) and unpredictable (clouds) component. The predictable component is significant so system operations with high solar penetrations could be designed with this in mind.

Because solar resources are better correlated with population centers and because public acceptance of solar in population centers is generally high, less transmission is needed to meet the same energy penetration from wind. The High-Solar Scenario required a little more than half the transmission needed for the High-Wind Scenario. In a transmission-constrained environment, such as what the United States is experiencing with low public acceptance for new transmission, solar provides significant benefits.

Next steps for WWSIS2 include production simulation modeling of the WI with wear-and-tear costs and emissions impacts of cycled and ramped fossil-fueled generation [14] for the four scenarios. Future work will include examination of mitigation options for retrofitting fossil-fueled generation to provide flexibility that helps to integrate more solar and wind power.

ACKNOWLEDGMENT

The authors acknowledge input from Michael Milligan, Sundar Venkataraman, Richard Piwko, Mark O'Malley, and other members of our Technical Review Committee.

This work was supported by the U.S. Department of Energy under Contract No. DE-AC36-08-GO28308 with the National Renewable Energy Laboratory.

REFERENCES

[1] L. Bird and M. Milligan, "Lessons from large-scale renewable energy integration studies," NREL/CP-6A20-54666, World Renewable Energy Forum Proceedings, Denver, CO, May 13–17, 2012.

[2] M. Milligan, E. Ela, D. Lew, D. Corbus, and Y. H. Wan, "Advancing wind integration study methodologies: Implications of higher levels of wind," NREL/CP-550-48944, WINDPOWER 2010 Proceedings, Dallax, TX, May 23–26.

[3] E. Ela, M. Milligan, B. Parsons, D. Lew, and D. Corbus, "Evolution of wind power integration studies: Past, present, and future," IEEE Power and Energy Society General Meeting Proceedings, Alberta, Calgary, Canada, July 26–30 2009.

[4] GE, Western Wind and Solar Integration Study, NREL/SR-550-47434, Golden, CO: National Renewable Energy Laboratory, 2010.

[5] N. Miller, K. Clark, G. Jordan, Z. Gao, and D. Lew, "Operational impacts of high solar penetrations in the Western U.S.," 1st International Workshop on Integration of Solar Power into Power Systems Proceedings, Aarhus, Denmark, Oct. 24, 2011.

[6] D. Lew, N. Miller, K. Clark, G. Jordan, and Z. Gao, Impact of High Solar Penetrations in the Western Interconnection, NREL/TP-5500-49667, Golden, CO: National Renewable Energy Laboratory, 2010.

[7] Western Electricity Coordinating Council, "Assumptions Matrix for the 2020 TEPPC Dataset," www.wecc.biz/library/StudyReport/Documents/Assumptions%20Matrix%20for%20the%202020%20TEPPC%20Dataset.pdf, 2010.

[8] D. Lew et al., "Wind data inputs for regional wind integration studies," IEEE Power and Energy Society General Meeting Proceedings, Detroit, MI, July 24–28, 2011.

[9] M. Hummon, E. Ibanez, G. Brinkman, D. Lew, "Sub-hour Solar Data for Power System Modeling from Static Spatial Variability Analysis," to be published the 2nd International Workshop on Integration of Solar Power in Power Systems Proceedings, Lisbon, Portugal, Nov. 12–13, 2012.

[10] P. Gilman and A. Dobos, System Advisor Model, SAM 2011.12.2: General Description, NREL/TP-6A20-53437, Golden, CO: National Renewable Energy Laboratory, 2012.

[11] C. Hansen, Validation of Simulated Irradiance and Power for the Western Wind and Solar Integration Study: Phase II, forthcoming, Sandia National Laboratories.

[12] 3TIER, Development of Regional Wind Resource and Wind Plant Output Datasets, NREL/SR-550-47676, Golden, CO: National Renewable Energy Laboratory, 2010.

[13] C. Potter, D. Lew, J. McCaa, S. Cheng, S. Eichelberger, and E. Grimit, "Creating the dataset for the Western Wind and Solar Integration Study (U.S.A.)," *Wind Engineering*, vol. 32, no. 4, pp. 325–338, 2008.

[14] W. Short et al., Regional Energy Deployment System (REEDS), NREL/TP-6A20-46534, Golden, CO: National Renewable Energy Laboratory, 2011.

[15] D. Lew, G. Brinkman, S. Lefton, N. Kumar, and D. Agan, "Impacts of wind and solar on fossil-fueled generators: Preprint," IEEE Power and Energy Society General Meeting Proceedings, San Diego, CA, July 22–26, 2012.

[16] Enernex, Eastern Wind Integration and Transmission Study (EWITS), NREL/SR-5500-47078, Golden, CO: National Renewable Energy Laboratory, 2010.

[17] E. Ibanez, G. Brinkman, M. Hummon and D. Lew, "A Solar reserve Methodology for Renewable Energy Integration Studies Based on Sub-Hourly Variability Analysis," to be published in the 2nd International Workshop on Integration of Solar Power in Power Systems Proceedings, Lisbon, Portugal, Nov. 12–13, 2012.